INTERNATIONAL JOURNAL OF COMPUTERS COMMUNICATIONS & CONTROL
ISSN 1841-9836, 13(4), 521-536, August 2018.

An Approach for Detecting Fault Lines in a Small Current Grounding System using Fuzzy Reasoning Spiking Neural P Systems

H. Rong, M. Ge, G. Zhang, M. Zhu

Haina Rong, Mianjun Ge, Gexiang Zhang*
School of Electrical Engineering
Southwest Jiaotong University
Chengdu, 610031, China
ronghaina@126.com, 641294684@qq.com, zhgxdylan@126.com
*Corresponding author: zhgxdylan@126.com

Ming Zhu
Chengdu University of Information Technology
Chengdu 610225, China
zhuming@126.com

Abstract: This paper presents a novel approach for detecting fault lines in a small current grounding system using fuzzy reasoning spiking neural P systems. In this approach, six features of current/voltage signals in a small current grounding system are analyzed by considering transient and steady components, respectively; a fault measure is used to quantify the possibility that a line is faulty; information gain degree is discussed to weight the importance of each of the six features; rough set theory is applied to reduce the features; and finally a fuzzy reasoning spiking neural P system is used to construct fault line detection models. Six cases in a small current grounding system prove the effectiveness of the introduced approach.
Keywords: Membrane computing; P system; spiking neural P systems; fault line detection; feature analysis; information gain degree; rough set theory

1 Introduction

As a rapidly developing branch of natural computing, membrane computing, initiated by Păun [3, 12], focuses on the investigations of a computational model, called a membrane system or a P system, abstracting from the structure and functioning of living cells, as well as from the way the cells are organized in tissues or high order structures. Numerous variants of P systems have Turing computing power [5, 15] or can solve computationally hard problems in a polynomial time [16, 26]. Inspired by the information processing principles in a living cell, a P system has certain characteristics, such as distribution, parallelism and expansibility, which make it suitable to solve a variety of practical problems [14, 46], such as engineering optimization [7, 28], languages generation [12, 40] and modeling biological and ecological systems [6].

In recent years, much attention is paid to spiking neural P systems (SN P systems), which were introduced in 2006 [5, 9] by considering the neurophysiological behavior of neurons sending electrical impulses (spikes) along axons from presynaptic neurons to postsynaptic neurons. Except for theoretical results [10, 13], SN P systems have been widely used to solve various application problems, such as combinatorial and engineering optimization problems [30, 38], signal recognition [2], arithmetic operations [17, 21, 28] and fuzzy knowledge representation [23]. Of a particular interest is the combination of SN P systems with fuzzy set theory, called fuzzy membrane computing [36], to solve fault diagnosis problems with respect to transformers [16, 42], transmission lines [8, 24, 25], traction power supply systems of high-speed railways [39] and metro

traction systems [10], in electric power systems. In general, there are two kinds of fuzzy reasoning spiking neural P systems (FRSN P systems) [36]: fuzzy reasoning spiking neural P system with real numbers (rFRSN P systems) [16] and fuzzy reasoning spiking neural P systems with trapezoidal fuzzy numbers (tFRSN P systems) [24].

The present work is motivated by two reasons. On the one hand, the application extension of FRSN P systems requires further discussions. On the other hand, the fault line detection in a small current grounding system is a very important problem and its detection accuracy needs to be enhanced [4, 9, 32, 35]. In China, most of medium-voltage distribution networks are small current grounding systems. Furthermore, about 70%–80% of the faults in distribution networks result from single-phase grounding. Therefore, the fault line detection problem with respect to single-phase grounding in a small current grounding system is a very common type of fault diagnosis in an electrical power system [1, 15, 30, 31]. Thus, a novel approach for detecting fault lines in a small current grounding system using FRSN P systems is proposed to enhance the accuracy. This approach first analyzes six features of current/voltage signals in a small current grounding system by considering transient and steady components, respectively. Then, the possibility that a line is faulty is quantified by using a fault measure. Next, information gain degree is used to weight the importance of each of the six features and rough set theory is discussed to reduce the features. Finally, FRSN P systems are used to construct fault line detection models. The effectiveness of the introduced approach is verified by several typical cases of fault line detection in a small current grounding system.

The organization of this article is as follows. Section 2 describes the fault line detection problem in a small current grounding system. Section 3 presents the proposed approach in detail. In Section 4, six typical cases are used to conduct the experiments. Conclusions are finally drawn in Section 5.

2 Problem description

In this paper, a 110kV/35kV distribution network with 6 feeders is considered. The simplified model of a distribution network is shown in Fig. 1. When a single-phase-to-ground fault occurs in the distribution network, any one of the 6 lines, 1–6, or the bus may be the faulty line. If the fault lasts for a long time, there will be much effect on the safe and stable operation of the distribution network, and even significant security incidents may happen, therefore, it is required to take a proper action to deal with the fault so as to restore power supply as soon as possible. When a line is faulty, the distribution network will generate zero sequence voltage and current. As usual, there means much difference in phase and amplitude of zero sequence current between the fault line and normal fault line.

Currently the widely used techniques are that a certain number of features are used to detect fault lines. There are three main techniques: steady state method, transient method and information fusion method. The steady state method is to select fault line by extracting the steady state fault characteristics of the distribution network, such as zero sequence current amplitude and phase, admittance, harmonic, power [1, 15, 30, 31]. But these fault characteristics are easily affected by the way of neutral point grounding and different fault grounding methods. With the development of signal processing technology, the transient component that contains a lot of fault information is considered to detect the fault line. In [41], the wavelet transform was used to extract the features from zero sequence current of each feeder and the fault line detection is realized by comparing the polarity. Wavelet analysis has a good characteristic of time-frequency localization and can decompose the signal into different frequency bands, so it is especially suitable for the analysis of non stationary signals and transient signals. In [27], a neural network was used to detect the fault line detection. In [47], a comprehensive fault line

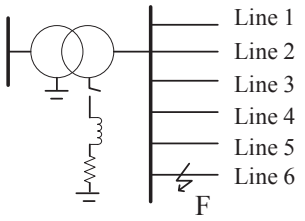

Figure 1: Simplified model of a distribution network

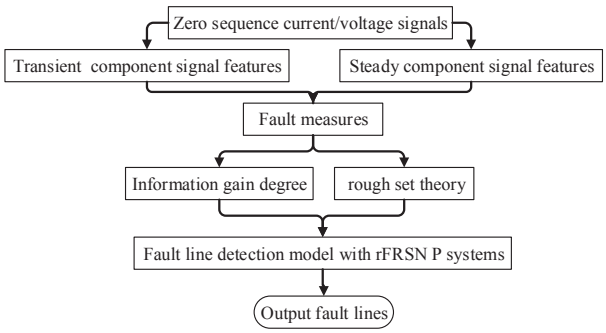

Figure 2: Framework of fault line detection approach

selection method based on fuzzy theory was discussed. In [14], an information fusion method based on D-S Evidence Theory was presented to detect fault lines in a small current grounding system.

3 The proposed approach

The fault line detection approach for a small current grounding system we propose here consists of four processes: feature analysis, fault measure calculation, feature information fusion and fault line detection model construction. Fig. 2 shows the framework of this approach. This paper considers both transient and steady components features of current or voltage signals. In the process of feature information fusion, the information gain degree is used to weight the importance of features and rough set theory is applied to reduce the features. A fault line detection model is constructed by using a fuzzy reasoning spiking neural P systems with real numbers (rFRSN P systems). In what follows, the processes will be described step by step.

3.1 Feature analysis

When a single-phase-to-ground fault occurs in the distribution network, the steady-state characteristics are mainly analyzed in the time domain. The fault current in the fault line is the ground capacitance current with the direction from the bus to the line, or it is the sum of the capacitance current in other lines with the direction from the line to the bus. The transient characteristics are analyzed in the frequency domain, including the amplitude, phase and energy of transient zero sequence current. To intuitively show the features, this study considers an example of a system, which has a single phase to ground fault at 0.02s, the transition resistance (R_0) is 0.2Ω, 20Ω, 2000Ω, representing the metal grounding, low impedance grounding and high impedance grounding, respectively. In the sequel, the first four features of steady components and the last two features of transient components are analyzed by using different methods, due to space limitations, this paper only gives a simulation diagram that the transition resistance

(R_0) is 0.2Ω.

(1) *Zero sequence current analysis*: when the neutral non-grounding system has a single phase grounding fault, the amplitude of the zero sequence current in the fault line equals the sum of the zero sequence currents in all the normal lines. The direction of the zero sequence current in the fault line is from the line to the bus and the direction of the zero sequence current in the normal line is from the bus to the line. Thus, if the amplitude of the zero sequence current in a line is equal to the sum of the amplitude of the zero sequence current in other lines, the direction is opposite to the other lines, which indicates that the line is a fault one. Fig. 3 shows the comparisons of zero sequence current between normal and fault lines, which refer to the lines in a neutral non-grounding system and a neutral grounding system, respectively.

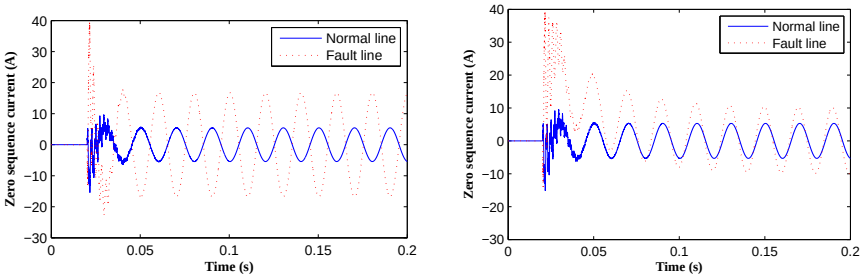

(a) Non-grounding system with $R_0 = 0.2\Omega$ (b) Grounding system with $R_0 = 0.2\Omega$

Figure 3: Zero sequence current comparisons between normal and fault lines

(2) *Zero-sequence reactive power analysis*: the zero sequence reactive power is the product of the corresponding zero sequence current and voltage. Fig. 4 shows the comparisons of zero sequence reactive power between normal and fault lines, which refer to the lines in a neutral non-grounding system and a neutral grounding system by using arc extinction coil, respectively. In the neutral non-grounding system, the zero sequence reactive component of the fault line is opposite to the zero sequence reactive component of the normal line, and its amplitude is bigger than that of the zero sequence reactive component of the normal line.

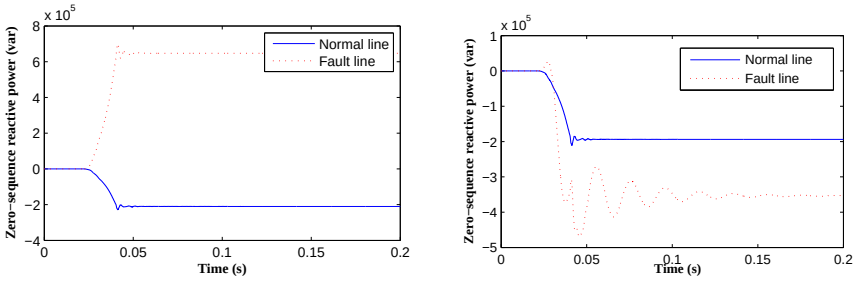

(a) Non-grounding system with $R_0 = 0.2\Omega$ (b) Grounding system with $R_0 = 0.2\Omega$

Figure 4: Zero sequence reactive power comparisons between normal and fault lines

(3) *Zero sequence admittance analysis*: In the neutral non-grounding system, the admittance angle of the normal line is in the first quadrant of the admittance plane angle, while

the admittance angle of the fault line is in the third quadrant. In the neutral grounding system by arc extinction coil, the admittance angles of the normal line and the fault line are in the first and second quadrant, respectively. Fig. 5 shows the comparisons of zero sequence admittance angles between normal and fault lines, which refer to the lines in a neutral non-grounding system and a neutral grounding system by using arc extinction coil, respectively.

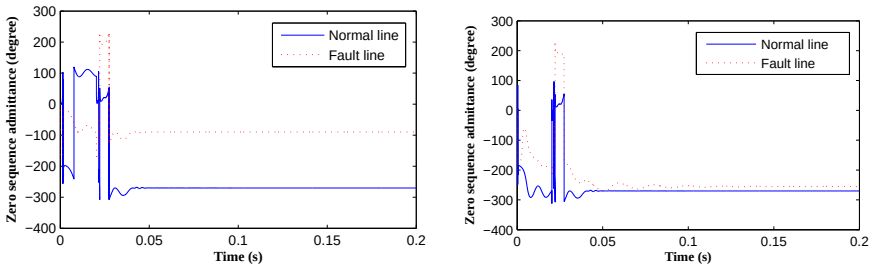

(a) Non-grounding system with $R_0 = 0.2\Omega$ (b) Grounding system with $R_0 = 0.2\Omega$

Figure 5: Zero sequence admittance angle comparisons between normal and fault lines

(4) *The fifth harmonic analysis*: the zero sequence current in a fault line contains a large number of odd harmonics, while the arc suppression coil will not greatly affect the magnitude and direction of the harmonic, so the harmonic can be used to detect the line. With the increase of harmonic frequency, the harmonic content becomes lower, so the fifth harmonic is usually used to realize fault line detection. Fig. 6 shows the comparisons of the fifth harmonic between normal and fault lines, which refer to the lines in a neutral non-grounding system and a neutral grounding system by using arc extinction coil, respectively.

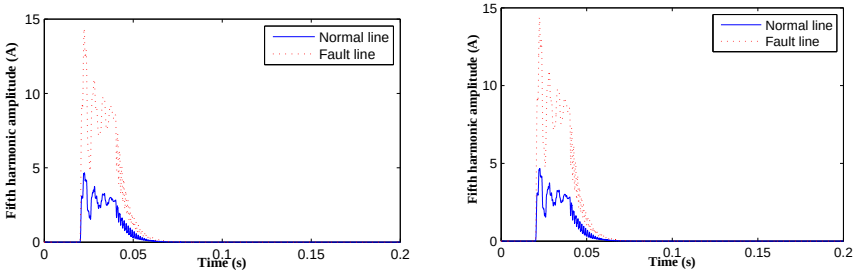

(a) Non-grounding system with $R_0 = 0.2\Omega$ (b) Grounding system with $R_0 = 0.2\Omega$

Figure 6: The fifth harmonic amplitude comparisons between normal and fault lines

(5) *Wavelet waveform analysis of zero sequence current*: the zero sequence current is decomposed into four layers by using wavelet transform, and the corresponding wavelet decomposition waveforms at scale 4 is shown in Fig. 7, where the waveforms in (a)–(f) are obtained from the neutral unearthed system and the figures (g)–(l) are gained from the neutral grounding system by using arc extinction coil. The wavelet energy polarity of the zero sequence current in the fault line is the opposite of the normal line, and the amplitude is the maximum. Thus, the fault line can be identified by comparing the energy

amplitude and polarity of the zero sequence current.

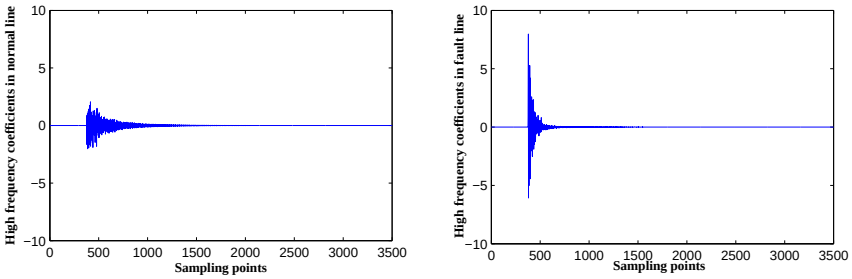

(a) Non-grounding system with $R_0 = 0.2\Omega$ (b) Grounding system with $R_0 = 0.2\Omega$

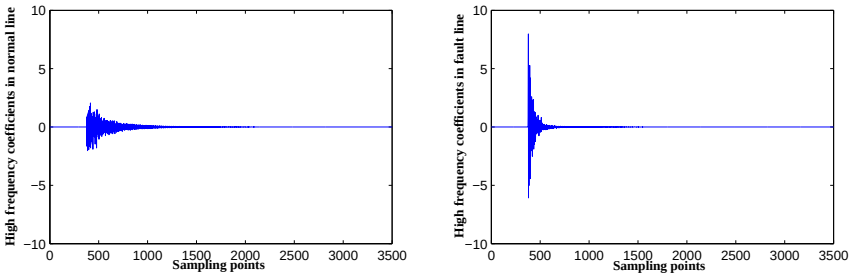

(a) Non-grounding system with $R_0 = 0.2\Omega$ (b) Grounding system with $R_0 = 0.2\Omega$

Figure 7: Wavelet waveform comparisons of zero sequence current between normal and fault lines

(6) *Transient zero sequence current analysis*: the direction and distribution of transient zero sequence currents shows similar phenomena to those of steady-state zero sequence currents. Fig. 8 show the comparisons of the products of zero sequence current between normal and fault lines, which refer to the lines in a neutral non-grounding system and a neutral grounding system by using arc extinction coil, respectively.

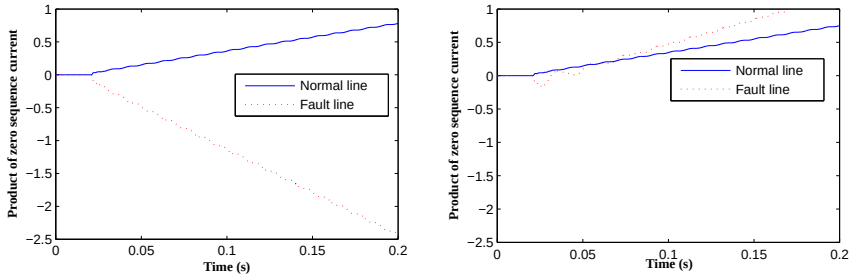

(a) Non-grounding system with $R_0 = 0.2\Omega$ (b) Grounding system with $R_0 = 0.2\Omega$

Figure 8: Comparisons of the products of zero sequence current between normal and fault lines

The analysis of the features discussed in this section indicates that there exists a difference between normal and fault lines so that the features can be used to detect the fault line in a small grounding system.

3.2 Fault measure

Following the feature analysis, a fault measure is discussed to quantify the possibility of a fault line [5, 33]. This article defines a fault measure as a real variable between 0 and 1. The smallest and biggest values 0 and 1 indicate that the line is normal and is faulty, respectively. Suppose that the number of lines in a distribution network is N and the number of fault line detection methods is H. The fault measure function is constructed by adopting line detection method h ($h = 1, 2, \ldots, N$) for line k ($k = 1, 2, \ldots, N$) is $X_h(k) = X_{rh}(k)X_{ah}(k)$, where $X_{rh}(k)$ is the relative fault measure function reflecting the difference of the fault measures between one line and the other lines in the distribution network; and $X_{ah}(k)$ is the reliability fault measure function reflecting the reliable degree of the fault measure.

As usual, different specific calculation methods are used for different fault features. To elaborate on the fault measure, we take the zero sequence current as an example. In a small current grounding system, the absolute values of the magnitudes of the zero sequence current in the fault line are equal to the sum of the absolute values of the amplitudes of all the normal lines. For line k, the magnitude of the zero sequence current is $|I_k|$. If $x = |I_k|/\sum_{n=1}^{N} |I_n|$ is big, the line tends to a fault line, conversely, the line is inclined to a normal one. The relative fault measure function of the line is described as follows:

$$X_{r1}(k) = \begin{cases} 1, & x \geq 0.5; \\ \frac{2N}{N-1}x - \frac{1}{N-1}, & \frac{1}{2N} < x < 0.5; \\ 0, & x \leq \frac{1}{2N}. \end{cases} \tag{1}$$

About the reliability fault measure function, when a single-phase-to-ground fault occurs in the system, the amplitudes of the zero sequence current in all lines reach to the maximum. If $x = |I_{max}|/\sum_{n=1}^{N} |I_n|$ is big, the fault characteristics of this method are obvious, on the contrary, they are not obvious. The reliability fault measure function of the line is described as follows:

$$X_{a1}(k) = \begin{cases} 1, & x \geq 0.5; \\ \frac{10N}{5N-6}x - \frac{6}{5N-6}, & \frac{3}{5N} < x < 0.5; \\ 0, & x \leq \frac{3}{5N}. \end{cases} \tag{2}$$

3.3 Information gain degree

Information gain degree is introduced to weight the importance of the six types of fault features in a small current grounding system. Suppose that X is the data for a particular sample group like the lines in this paper and A is the attribute set for the fault line detection methods, $A = \{H_1, H_2, \ldots, H_m\}$. The lines are divided into two types: fault and normal ones. So $X = \{X_1, X_2\}$, where $|X_i|$ is the number of sample instances of class i and $|X|$ is the total number of sample instances of X.

If $H(X_i)$ is the probability that a sample instance belongs to class i, then $H(X_i) = |X_i|/|X|$. Assume that $M(X)$ is the degree of uncertain information about X and it is $\sum_{i=1}^{m}[-H(X_i)\log_2 H(X_i)]$, where method H has the characters $h_1, h_2, \ldots, h_j$. In the case of $H = h_j$, C_{ij} is the number of sample instances of class i and Y_j is the total number of sample instances, thus, the probability $H(X_i|H = h_j)$ is $C_{ij}/|Y_i|$, the conditional entropy of H and the classification information entropy are described as $M(X, H = h_j) = \sum_j[-H(X_i|H = h_j)\log_2 H(X_i|H = h_j))]$,

and $B(X,H) = \sum_j [H(X_i|H = h_j)M(X, H = h_j)]$. The information gain of H is $\Delta Q_h = M(X) - B(X,H) = M(X) - \sum_j [H(X_i|H = h_j)M(X, H = h_j)]$. The information gain degree is normalized and the weight of the line detection method is $X_{mh}(k) = \Delta Q_h / \Sigma \Delta Q$.

3.4 Rough set theory

In this study, rough set theory is used to reduce the fault features in a small current grounding system. Rough set theory is a tool to analyze the incomplete and imprecise data [24, 43]. It is used to simplify the rule reduction to information system. The main ideas of rough set theory include knowledge reduction and domain reduction, which are described in a very brief way as follows. Knowledge reduction: suppose that R is an equivalence relation, $ind(R)$ represents the intersection of all the equivalence relations in R, $r \in R$. If $ind(R) = ind(R - \{r\})$, then r can be omitted, otherwise, r cannot be omitted. Domain reduction: suppose that $F = \{X_1, X_2, \ldots, X_n\}$ is a set family, $X_j \in U$ (U represents the domain). If $\bigcap(F - \{X_i\}) = \bigcap F$, then X_i can be omitted, domain reduction can delete the same decision rules and redundant attribute values in an information system so as to obtain the minimal solution.

In this paper, the condition attributes are the fault line detection methods and the decision attribute decides whether a fault detection method corresponding to a kind of features is correct or not. Conditional attributes require to be discretized. Thus, this method is used to simplify the condition attributes and eliminate some unnecessary condition attributes and redundant decision rules. Finally, the decisive solution is obtained.

3.5 Fault line detection models with rFRSNPS

In this section, a fuzzy reasoning spiking neural P system with real numbers (rFRSNPS) [16] is used to build the fault line detection model. The definition of rFRSN P system is first briefly described. Subsequently, the reasoning algorithm and fuzzy production rules of fault line detection are discussed. Finally, the fault line detection model is presented.

Fuzzy reasoning Spiking neural P systems

The definition and reasoning algorithm of rFRSNPS is described in [16], due to space limitations, this paper no longer gives a specific process.

Fuzzy production rules of fault line detection

The rFRSN P systems contain two types of neurons: proposition neurons and rule neurons, the rule neurons also express the fuzzy production rules. In this paper, we will describe three different kinds of fault line selection rules for rFRSN P system.

(1) (*General Rules*) R_i ($CF = c_i$): IF $p_j(\theta_j)$ THEN $p_k(\theta_k)$, where p_j and p_k represent propositions, c_i represents the certainty factor of rule R_i, as a real number belonging to [0,1], θ_j and θ_k are real numbers in [0,1] representing the truth values of p_j and p_k, the truth value of p_k is calculated as $\theta_k = \theta_j * c_i$

(2) (*And Rules*) R_i ($CF = c_i$): IF $p_1(\theta_1)$ and ... and $p_{k-1}(\theta_{k-1})$ THEN $p_k(\theta_k)$, where p_1, ... p_k are proposition, c_i represents the certainty factor of rule R_i, as a real number belonging to [0,1], θ_1, ... θ_k are real numbers in [0,1] representing the truth values of p_1, ... p_k, the truth value of p_k is calculated as $\theta_k = min(\theta_1, \ldots, \theta_{k-1}) * c_i$.

(3) (*Or Rules*) R_i ($CF = c_i$): IF $p_1(\theta_1)$ or ... or $p_{k-1}(\theta_{k-1})$ THEN $p_k(\theta_k)$, where p_1, ... p_k are proposition, c_i represents the certainty factor of rule R_i, as a real number belonging to [0,1], θ_1, ... θ_k are real numbers in [0,1] representing the truth values of p_1, ... p_k, the truth value of p_k is calculated as $\theta_k = max(\theta_1, \ldots, \theta_{k-1}) * c_i$.

Fault line detection model

Based on the fuzzy production rules of fault line detection discussed above, we can establish the fault line detection model with rFRSNPS for a line. The model is shown in Fig. 9, where b, c, d, f and P_1 represent the fault line measure values of the zero sequence current phase, the zero sequence reactive power, the zero sequence admittance amplitude, the transient zero sequence current and fused fault measure, respectively. The rFRSNPS for fault line detection is described as follows:

$$\Pi_1 = (O, \sigma_1, \sigma_2, \ldots, \sigma_{18}, syn, in, out)$$

where

(1) O=$\{a\}$ is the singleton alphabet (a is called spike);

(2) $\sigma_1, \ldots, \sigma_{11}$ are proposition neurons corresponding to the propositions with fuzzy truth values $\theta_1, \ldots, \theta_{11}$;

(3) $\sigma_{12}, \ldots, \sigma_{18}$ are rule neurons, where σ_{12}, σ_{15} are *general* rule neurons; σ_{16}, σ_{17} are *and* rule neurons; σ_{18} are *or* rule neurons;

(4) $syn = \{(1,12), (2,13), (3,14), (4,15), (5,16), (5,17), (6,16), (7,17), (8,16), (8,17), (9,18), (10,18), (12,5), (13,6), (14,7), (15,8), (16,9), (17,10), (18,11),\}$;

(5) in=$\{\sigma_1, \ldots, \sigma_4\}$;

(6) out=$\{\sigma_{11}\}$.

4 Case studies

The distribution network system shown in Fig. 1 is simulated on MATLAB/Simulink to obtain training and testing samples for verifying the fault line detection. The transformer ratio is 110kV/35kV. The simulation time is 0.2s. The lines length are 10km, 15km, 20km, 28km, 35km, 50km, respectively, the positive sequence parameters of line are $0.17ohms/km$, $1.21mH/km$ and 36.6+j$172F/km$, the zero sequence parameters of line are $0.23ohms$, $5.48mH/km$ and $6pF/km$. In the neutral ungrounded system, the testing samples are considered for several values of fault initial phase(0, 45 and 90 degrees), fault location(10%, 50% and 90% of lines 1 to 6) and transition resistance(0.2, 20 and 2000 ohms).

In the process of the simulation experiment, we collect 162 features from each of lines 1 to 6 and totally 972 zero sequence signal features as data sets. Next, the fault line measure values of the zero sequence current amplitude, the zero sequence current phase, the zero sequence reactive power, the zero sequence admittance amplitude, the wavelet energy of zero sequence current and the transient zero sequence current can be calculated by using the zero sequence signal. In what follows, six cases in the small current grounding system are used to test the introduced approach.

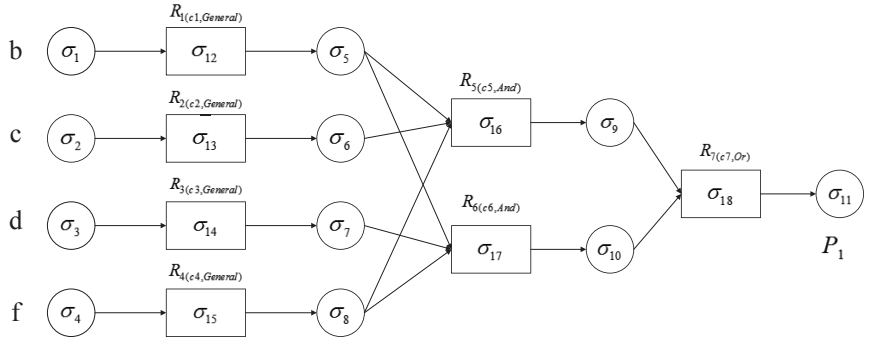

Figure 9: A certain line of fault line selection model with rFRSNPS

Case 1: single-phase-to-ground fault occurring in line 1: initial phase is 90 degrees; the fault is located at 90% of the line; transition resistance is 20 ohms.

Table 1 gives fault measure values of zero sequence current signals in lines 1–6. Then, the values between 0∼0.3, 0.3∼0.7 and 0.7∼1 are discretized as 0, 1, and 2, respectively. The results are shown in Table 2. Next, Eqs. subsection 3.3 are used to compute the weights of the six feature analysis methods and the results are 0.4833, 0.6500, 0.6500, 0.4833, 0.6500 and 0.6500, respectively. Subsequently, rough set theory is applied to reduce the condition attributes consisting of the features shown in Table 1. The reduced result is (b∧f∧(c∨d)), where b and f are the core attributes. Finally, the reasoning algorithm described above and fault line detection model with rFRSNPS are used to obtain the detection result. The detailed steps are described as follows:

Step 1: $g = 0$, $\boldsymbol{\theta}_0 = (0.9583, 0.9667, 0.6467, 0.9439, 0, 0, 0, 0, 0, 0, 0,)^T$,
$\boldsymbol{C} = diag(0.6500, 0.6500, 0.4833, 0.6500, 1, 1, 1)$,$\boldsymbol{\delta}_0 = 0$.

$$\boldsymbol{D}_1 = \begin{bmatrix} \boldsymbol{A}_1 & 0 \\ 0 & 1 \end{bmatrix}_{11\times7} \quad \boldsymbol{D}_2 = \begin{bmatrix} 0 & 0 \\ 0 & \boldsymbol{A}_2 \\ 0 & 0 \end{bmatrix}_{11\times7} \quad \boldsymbol{D}_3 = \begin{bmatrix} 0 & 0 \\ 0 & \boldsymbol{A}_3 \end{bmatrix}_{11\times7} \quad \boldsymbol{E}^T = \begin{bmatrix} 0 \\ \boldsymbol{B}_1 \end{bmatrix}_{11\times7}$$

$$\boldsymbol{A}_1 = \begin{bmatrix} 1 & 0 & 0 & 0 \\ 0 & 1 & 0 & 0 \\ 0 & 0 & 1 & 0 \\ 0 & 0 & 0 & 1 \end{bmatrix}_{4\times4} \quad \boldsymbol{A}_2 = \begin{bmatrix} 1 & 1 & 0 \\ 1 & 0 & 0 \\ 0 & 1 & 0 \\ 1 & 1 & 0 \end{bmatrix}_{4\times3} \quad \boldsymbol{A}_3 = \begin{bmatrix} 0 & 1 \\ 0 & 1 \\ 0 & 0 \end{bmatrix}_{3\times2} \quad \boldsymbol{B}_1 = \begin{bmatrix} 0 & 0 & 0 & 0 & 0 & 0 & 1 \\ 0 & 0 & 0 & 0 & 0 & 1 & 0 \\ 0 & 0 & 0 & 0 & 1 & 0 & 0 \\ 0 & 0 & 0 & 1 & 0 & 0 & 0 \\ 0 & 0 & 1 & 0 & 0 & 0 & 0 \\ 0 & 1 & 0 & 0 & 0 & 0 & 0 \\ 1 & 0 & 0 & 0 & 0 & 0 & 0 \end{bmatrix}_{7\times7}$$

Step 2: The firing condition of proposition neuron is satisfied and there is a postsynaptic rule neuron, so the proposition neuron fires and transmits a spike to the next rule neuron by the directed arc.

Step 3: $\boldsymbol{\delta}_{g+1} = (\boldsymbol{D}_1^T \otimes \boldsymbol{\theta}_g) + (\boldsymbol{D}_2^T \oplus \boldsymbol{\theta}_g) + (\boldsymbol{D}_3^T \odot \boldsymbol{\theta}_g)$, $\boldsymbol{\delta}_1 = (0.9583, 0.9667, 0.6467, 0.9439, 0, 0, 0)^T$.

Step 4: $\boldsymbol{\delta}_1 \neq 0$. The reasoning algorithm continues.

Step 5: $g = 1$.

Step 6: $\boldsymbol{\theta}_g = \boldsymbol{E}^T \odot (D \otimes \boldsymbol{\delta}_g)$, $\boldsymbol{\theta}_1 = (0, 0, 0, 0, 0.6229, 0.6284, 0.3126, 0.6135, 0, 0, 0)^T$.

Step 7: $\boldsymbol{\delta}_{g+1} = (\boldsymbol{D}_1^T \otimes \boldsymbol{\theta}_g) + (\boldsymbol{D}_2^T \oplus \boldsymbol{\theta}_g) + (\boldsymbol{D}_3^T \odot \boldsymbol{\theta}_g)$, $\boldsymbol{\delta}_2 = (0, 0, 0, 0, 0.6135, 0.3126, 0)^T$.

Step 8: $\boldsymbol{\delta}_2 \neq 0$. The reasoning algorithm continues.

Step 9: $g = 2$.

Step 10: $\boldsymbol{\theta}_g = \boldsymbol{E}^T \odot (D \otimes \boldsymbol{\delta}_g)$, $\boldsymbol{\theta}_2 = (0, 0, 0, 0, 0, 0, 0, 0, 0.6135, 0.3126, 0)^T$.

Step 11: $\boldsymbol{\delta}_{g+1} = (\boldsymbol{D}_1^T \otimes \boldsymbol{\theta}_g) + (\boldsymbol{D}_2^T \oplus \boldsymbol{\theta}_g) + (\boldsymbol{D}_3^T \odot \boldsymbol{\theta}_g)$, $\boldsymbol{\delta}_3 = (0, 0, 0, 0, 0, 0, 0.6135)^T$.

Table 1: Fault measure values of zero sequence current signals in lines 1–6,
where CA, CP, RP, AA, WE and TC represent current amplitude, current phase, reactive power, admittance amplitude, wavelet energy and transient current, respectively.

line	CA	CP	RP	AA	WE	TC
1	0.4371	0.9583	0.9667	0.6467	0.9182	0.9439
2	0.0675	0.0167	0.4234	0.3175	0.0483	0.3203
3	0.0945	0.1083	0.1092	0.0945	0.2531	0.0000
4	0.0506	0.3917	0.0823	0.0506	0.0658	0.0000
5	0.1182	0.1518	0.3167	0.3182	0.2146	0.0186
6	0.3691	0.2417	0.2631	0.1694	0.0731	0.3034

Table 2: Discretized fault measure values,
where CA, CP, RP, AA, WE and TC represent current amplitude, current phase, reactive power, admittance amplitude, wavelet energy and transient current, respectively.

line	CA	CP	RP	AA	WE	TC
1	1	2	2	1	2	2
2	0	0	1	1	0	1
3	0	0	0	0	0	0
4	0	1	0	0	0	0
5	0	0	1	1	0	0
6	1	0	0	0	0	1

Step 12: $\boldsymbol{\delta}_3 \neq 0$. The reasoning algorithm continues.

Step 13: $g = 3$.

Step 14: $\boldsymbol{\theta}_g = \boldsymbol{E}^T \odot (D \otimes \boldsymbol{\delta}_g)$, $\boldsymbol{\theta}_3 = (0,0,0,0,0,0,0,0,0,0,0.6135)^T$.

Step 15: $\boldsymbol{\delta}_{g+1} = (\boldsymbol{D}_1^T \otimes \boldsymbol{\theta}_g) + (\boldsymbol{D}_2^T \oplus \boldsymbol{\theta}_g) + (\boldsymbol{D}_3^T \odot \boldsymbol{\theta}_g)$, $\boldsymbol{\delta}_4 = (0,0,0,0,0,0,0)^T$.

Step 16: $\boldsymbol{\delta}_4 = 0$. The reasoning algorithm ends. The reasoning result can be obtained from output neuron P_1. The pulse value of the spike in P_1 is $0.6135(> 0.5)$. The rest may be inferred in the same way. The reasoning results of the other five lines can also be obtained and the pulse values of the spike in P_2 to P_6 are 0.0109, 0, 0, 0.0121, $0.1571(< 0.2)$, respectively. So line 1 is the fault line.

Case 2: single-phase-to-ground fault occurring in line 2: initial phase is 90 degrees; the fault is located at 90% of the line; transition resistance is 20 ohms.

Similar to *Case 1*, the weights of the six feature analysis methods are 0.4833, 0.6500, 0.6500, 0.4971, 0.6500 and 0.6500, respectively. The reduced result is (c∧f∧(b∨d)), where c and f are the core attributes. The initial parameter matrices of rFRSNPS for fault line detection are as follows:

$\boldsymbol{\theta}_0 = (0.9252, 0.9321, 0.7172, 0.9986, 0, 0, 0, 0, 0, 0, 0)^T$,

$\boldsymbol{C} = diag(0.6500, 0.6500, 0.4971, 0.6500, 1, 1, 1)$, $\boldsymbol{\delta}_0 = 0$.

According to the reasoning algorithm, we can get:

$\boldsymbol{\theta}_1 = (0,0,0,0,0.6014, 0.6059, 0.3565, 0.6491, 0, 0, 0)^T$,

$\boldsymbol{\theta}_2 = (0,0,0,0,0,0,0,0,0.6014, 0.3565, 0)^T$,

$\boldsymbol{\theta}_3 = (0,0,0,0,0,0,0,0,0,0,0.6014)^T$, and $\boldsymbol{\delta}_4 = 0$.

So, the pulse value of the spike in P_2 is 0.6014 (> 0.5). The pulse values of the spike in P_1, P_3, P_4, P_5 and P_6 are 0.1109, 0.0251, 0.0459, 0 and 0.0241 (< 0.2), respectively. Thus, line 2 is the fault line.

Case 3: single-phase-to-ground fault occurring in line 3: initial phase is 90 degrees; the fault is located at 90% of the line; transition resistance is 2000 ohms.

Similarly, the weights of the six feature analysis methods are 0.1909, 0.6500, 0.6500, 0.4833, 0.6500 and 0.6500, respectively. The reduced result is (b∧c∧(d∨e∨f)), where b and c are the core attributes; e is the fault measure value of the wavelet energy of zero sequence current. The initial parameter matrices of the rFRSNPS for fault line selection are as follows:

$\boldsymbol{\theta}_0 = (0.9167, 0.8723, 0.6842, 0.5974, 0.8783, 0, 0, 0, 0, 0, 0, 0, 0)^T$,

$\boldsymbol{C} = diag(0.6500, 0.6500, 0.4833, 0.6500, 0.6500, 1, 1, 1, 1)$, $\boldsymbol{\delta}_0 = 0$.

According to the reasoning algorithm, we can get:

$\boldsymbol{\theta}_1 = (0,0,0,0,0,0.5959,0.5670,0.3307,0.3883,0.5709,0,0,0,0)^T$,

$\boldsymbol{\theta}_2 = (0,0,0,0,0,0,0,0,0,0,0.3307,0.3883,0.5670,0)^T$,

$\boldsymbol{\theta}_3 = (0,0,0,0,0,0,0,0,0,0,0,0,0,0.5670)^T$, and $\boldsymbol{\delta}_4 = 0$.

Thus, the pulse value of the spike in P_3 is 0.5670 (> 0.5). The pulse values of the spike in P_1, P_2, P_4, P_5 and P_6 are 0.0705, 0.1308, 0, 0.0090 and 0.1588 (< 0.2), respectively. So line 3 is the fault line.

Case 4: single-phase-to-ground fault occurring in line 4: initial phase is 0 degrees; the fault is located at 90% of the line; transition resistance is 2000 ohms.

The weights of the six feature analysis methods are 0.1909, 0.6500, 0.6500, 0.4971, 0.6500, 0.6500. The reduced result is (b∧f∧(c∨d)), where b and f are the core attributes. The initial parameter matrices of the rFRSNPS for fault line selection are as follows:

$\boldsymbol{\theta}_0 = (0.8918, 0.8816, 0.5999, 0.8871, 0, 0, 0, 0, 0, 0, 0)^T$,

$\boldsymbol{C} = diag(0.6500, 0.6500, 0.4971, 0.6500, 1, 1, 1)$, $\boldsymbol{\delta}_0 = 0$.

According to the reasoning algorithm, we can get:

$\boldsymbol{\theta}_1 = (0,0,0,0,0.5797,0.5730,0.2982,0.5766,0,0,0)^T$,

$\boldsymbol{\theta}_2 = (0,0,0,0,0,0,0,0,0.5730,0.2982,0)^T$,

$\boldsymbol{\theta}_3 = (0,0,0,0,0,0,0,0,0,0,0.5730)^T$, and $\boldsymbol{\delta}_4 = 0$.

So the pulse value of the spike in P_4 is 0.5730(> 0.5). The pulse values of the spike in P_1, P_2, P_3, P_5 and P_6 are 0.0644, 0.0203, 0.1860, 0.0164 and 0.0005 (< 0.2), respectively. Thus, line 4 is the fault line.

Case 5: single-phase-to-ground fault occurring in line 5: initial phase is 0 degrees; the fault is located at 50% of the line; transition resistance is 20 ohms.

The weights of the six feature analysis methods are 0.4833, 0.6500, 0.6500, 0.4833, 0.6500, 0.6500. The reduced result is (f∧e∧(b∨c)∧(c∨d)), where f and e are the core attributes. The initial parameter matrices of the rFRSNPS for fault line selection are as follows:

$\boldsymbol{\theta}_0 = (0.8866, 0.9167, 0.6879, 0.9336, 1, 0, 0, 0, 0, 0, 0, 0, 0)^T$,

$\boldsymbol{C} = diag(0.6500, 0.6500, 0.4833, 0.6500, 0.6500, 1, 1, 1, 1))$, $\boldsymbol{\delta}_0 = 0$.

According to the reasoning algorithm, we can get:

$\boldsymbol{\theta}_1 = (0,0,0,0,0,0.5763,0.5959,0.3325,0.6069,0.6500,0,0,0,0)^T$,

$\boldsymbol{\theta}_2 = (0,0,0,0,0,0,0,0,0,0,0.5764,0.3325,0.3325,0)^T$,

$\boldsymbol{\theta}_3 = (0,0,0,0,0,0,0,0,0,0,0,0,0,0.5764)^T$, and $\boldsymbol{\delta}_4 = 0$.

So the pulse value of the spike in P_5 is 0.5730 (> 0.5). The pulse values of the spike in P_1, P_2, P_3, P_4 and P_6 are 0.0283, 0, 0.1528, 0 and 0.0664 (< 0.2), respectively. Thus, line 5 is the fault line.

Case 6: single-phase-to-ground fault occurring in line 6: initial phase is 0 degrees; the fault is located at 10% of the line; transition resistance is 20 ohms.

The weights of the six feature analysis methods are 0.4833, 0.6500, 0.6500, 0.4833, 0.6500, 0.6500. The reduced result is (b∧c∧f∧(e∨d)), where b, c and f are the core attributes. The initial parameter matrices of the rFRSNPS for fault line selection are as follows:

$\boldsymbol{\theta}_0 = (0.9284, 0.8987, 0.5847, 0.9312, 0.9021, 0, 0, 0, 0, 0, 0, 0, 0)^T$,

$\boldsymbol{C} = diag(0.6500, 0.6500, 0.4833, 0.6500, 0.6500, 1, 1, 1, 1))$, $\boldsymbol{\delta}_0 = 0$.

According to the reasoning algorithm, we can get:

$\boldsymbol{\theta}_1 = (0, 0, 0, 0, 0, 0.6035, 0.5842, 0.2826, 0.6053, 0.5864, 0, 0, 0)^T$,

$\boldsymbol{\theta}_2 = (0, 0, 0, 0, 0, 0, 0, 0, 0, 0, 0.2826, 0.5842, 0)^T$,

$\boldsymbol{\theta}_3 = (0, 0, 0, 0, 0, 0, 0, 0, 0, 0, 0, 0, 0, 0.5842)^T$, and $\boldsymbol{\delta}_4 = 0$.

So the pulse value of the spike in P_6 is 0.5842 (> 0.5). The pulse values of the spike in P_1, P_2, P_3, P_4 and P_5 are 0.1083, 0.0613, 0, 0.0328 and 0.0871 (< 0.2), respectively. Thus, line 6 is the fault line.

The experimental results of the six cases in a small grounding system indicate that the proposed fault line detection approach is not affected by fault locations, fault resistance and fault closing angles.

5 Conclusions

In this paper, a novel approach is introduced by fuzzy reasoning spiking neural P systems to detect fault lines in a small current grounding system. The feature analysis is performed on steady and transient components of zero sequence current of a small current grounding system. Steady state features consist of zero sequence current signal amplitudes, zero-sequence reactive power, zero sequence admittance and the fifth harmonic. Transient features are composed of wavelet energy of zero sequence current and transient zero sequence current signal amplitudes. Experiments conducted on several cases of a distribution network system verify the feasibility and correctness of the presented approach. Future work will focus on the improvement of the fault line detection accuracy and the reliability of results. Following this work, micro grids and smart grids will be also considered in the future study.

Acknowledgment

This work was supported by National Natural Science Foundation of China (61672437, 61702428) and by Sichuan Science and Technology Program (2018GZ0185, 2018GZ0085, 2017GZ0159).

Bibliography

[1] Chen, Z.L.; Fan, C.J. (2006); Fault line selection for small current neutral grounding system based on the fifth harmonic current mutation in distribution system, *Proc. CSEE*, 18(5), 37–40, 2006.

[2] Chen, Z.; Zhang, P.; Wang, X.; Shi, X.; Wu, T.; Zheng, P. (2016); A computational approach for nuclear export signals identification using spiking neural P systems, *Neural Comput Appl*, 29(3), 695–705, 2016.

[3] Dzitac, I. (2015); Impact of membrane computing and P systems in ISI WoS. Celebrating the 65th birthday of Gheorghe Păun, *International Journal of Computers Communications & Control*, 10(5): 617-626, 2015.

[4] Dong, X.; Shi, S. (2008); Identifying single-phase-to-ground fault feeder in neutral non effectively grounded distribution system using wavelet transform, *IEEE Trans on Power Deliver*, 23(4), 1829–1837, 2008.

[5] Fan, L. P.; Yuan, Z.Q.; Zhang, K. (2009); System with insulated neutral point earthing of fault line detection fusion technology study based on fuzzy and rough set theory, *Central China Electric Power*, 1, 7–11, 2009.

[6] Frisco, P.; Gheorghe, M.; Pérez-Jiménez, M.J. (Eds.) (2014); *Applications of membrane computing in systems and synthetic biology*, Springer, Heidelberg, 2014.

[7] He, J., Xiao, J., Liu, X., Wu, T., Song, T. (2015); A novel membrane-inspired algorithm for optimizing solid waste transportation, *Optik*, 126(23), 3883–3888, 2015.

[8] Huang, K.; Wang, T.; He, Y.; Zhang, G.; Pérez-Jiménez, M. J. (2016); Temporal fuzzy reasoning spiking neural P systems with real numbers for power system fault diagnosis, *J Comput Theor Nanosci*, 13(6), 3804–3814, 2016.

[9] Huang, T.; Voronca, S. L.; Purcarea, A.; Estebsari, A.; Bompard, E. (2014); Analysis of chain of events in major historic power outages, *Adv Electr Comput Eng*, 14(3), 63-70, 2014.

[10] He, Y.; Wang, T.; Huang, K.; Zhang, G.; Pérez-Jiménez, M.J. (2015); Fault diagnosis of metro traction power systems using a modified fuzzy reasoning spiking neural P system, *Rom J Inf Sci Technol*, 18(3), 256–272, 2015.

[11] Ionescu, M.; Păun, Gh.; Yokomori, T. (2006); Spiking neural P systems, *Fund Inform*, 71(2-3), 279–308, 2006.

[12] Jiang, K.; Chen, W.; Zhang, Y.; Pan, L. (2016); On string languages generated by sequential spiking neural P systems based on the number of spikes, *Nat Comput*, 15(1), 87–96, 2016.

[13] Jiang, K.; Pan, L. (2016); Spiking neural P systems with anti-spikes working in sequential mode induced by maximum spike number, *Neurocomputing*, 171, 1674–1683, 2016.

[14] Jia, Q.; Shi, L.; Wang, N.; Dong, H. (2012); A fusion method for ground fault line detection in compensated power networks based on evidence theory and information entropy, *Trans China Electrotech Soc*, 27(6): 191–197, 2012.

[15] Liang, R.; Xin, J.; Wang, C.L.; Li, G.X.; Tang, J.J. (2010); Fault line selection in small current grounding system by improved active component method, *High Voltage Eng*, 36(2), 375–379, 2010.

[16] Liu, X.; Li, Z.; Suo, J.; Liu, J.; Min, X. (2015); A uniform solution to integer factorization using time-free spiking neural P system, *Neural Comput Appl*, 26(5): 1241–1247, 2015.

[17] Liu, X.; Li, Z.; Liu, J.; Liu, L.; Zeng, X. (2015); Implementation of arithmetic operations with time-free spiking neural P systems, *IEEE Trans on Nanobiosci*, 14(6), 617–624, 2015.

[18] Păun, Gh. (2000); Computing with membranes, *J Comput System Sci*, 61(1), 108–143, 2000.

[19] Păun, Gh. (2016); Membrane computing and economics: A general view, *International Journal of Computers Communications & Control*, 11(1), 105-112, 2016.

[20] Păun, Gh.; Rozenberg, G.; Salomaa, A. (Eds.) (2010); *The Oxford handbook of membrane computing*, Oxford University Press, New York, 2010.

[21] Peng, H.; Wang, J.; Pérez-Jiménez, M.J.; Wang, H.; Shao, J.; Wang, T. (2013); Fuzzy reasoning spiking neural P system for fault diagnosis, *Inform Sciences*, 235(20), 106–116, 2013.

[22] Pan, L.; Păun, Gh. (2009); Spiking neural P systems with anti-spikes, *International Journal of Computers Communications & Control*, 4(3), 273–282, 2009.

[23] Pan, L.; Păun, Gh.; Zhang, G.; Neri, F. (2017); Spiking neural P systems with communication on request, *Int J Neural Syst*, 27(8), 1750042, 2017.

[24] Pawlak, Z. (1998); Rough set theory and its applications to data analysis, *Cybernet Syst*, 29(7), 661–688, 1998.

[25] Rong, H.; Zhu, M.; Feng, Z.; Zhang, G.; Huang, K. (2017); A novel spproach to fault classification of power transmission lines using singular value decomposition and fuzzy reasoning spiking neural P systems, *Rom J Inf Sci Technol*, 20(1), 18-31, 2017.

[26] Song, B.; Pérez-Jiménez, M.J.; Pan, L. (2015); Computational efficiency and universality of timed P systems with membrane creation, *Soft Comput*, 19(11), 3043–3053, 2015.

[27] Shu, H.; Qiu, G.; Li, C.; Peng, S. (2010); A fault line selection algorithm using neural network based on S-transform energy, *Proc. 6th Internat Conf Nat Comput*, 3, 1478–1482, 2010.

[28] Song, T.; Zheng, H.; Juanjuan (2014); Solving vertex cover problem by tissue P systems with cell division, *Appl Math Inf Sci*, ISSN 2325-0399, 8(8), 333-337, 2014.

[29] Song, T.; Zheng, P.; Wong, M. L. D.; Wang, X. (2016); Design of logic gates using spiking neural P systems with homogeneous neurons and astrocytes-like control, *Inform Sciences*, 372, 380-391, 2016.

[30] Sang, Z.; Pan, Z.; Li, L.; Zhang, H. (1997); A new approach of fault line identification, fault distance measurement and fault location for single phase-to-ground fault in small current neutral grounding system, *Power Syst Technol*, 21(10), 50–52, 1997.

[31] Tang, Y.; Chen, K.; Chen, Q.; Dong, H.B. (2005); Study on earthed fault location method in indirectly grounding power system using maximum value of absolute value summation of measurement admittance mutual difference, *Proc. CSEE* , 25(6), 49–54, 2005.

[32] Voronca, S. L.; Voronca, M. M.; Huang, T.; Purcărea, A. A. (2015); Applying the analytic hierarchy process to rank natural threats to power system security, *U P B Sci Bull Ser C*, 77(3), 269-280, 2015.

[33] Wang, B.; Yu, C.K.; Ye, J.; Bai, Y. (2011); Fault line selection method for single phase-to-ground faults of multi-criteria information integrated with lower current grounding power system based on fuzzy theory, *Guangdong Electric Power*, 9, 24–28, 2011.

[34] Wang, J.; Shi, P.; Peng, H.; Pérez-Jiménez, M.J.; Wang, T. (2013); Weighted fuzzy spiking neural P systems, *IEEE Trans on Fuzzy Syst*, 21(2), 209–220, 2013.

[35] Welfonder, T.; Leitloff, V.; Fenillet, R.; Vitet, S. (2000); Location strategies and evaluation of detection algorithms for earth faults in compensated MV distribution systems, *IEEE Trans on Power Deliver*, 15(4), 1121–1128, 2000.

[36] Wang, T.; Zhang, G.; Pérez-Jiménez, M.J.(2015); Fuzzy membrane computing: theory and applications, Solving vertex cover problem by tissue P systems with cell division, *International Journal of Computers Communications & Control*, 10(6), 144–175, 2015.

[37] Wang, T.; Zhang, G.; Zhao, J.; He, Z.; Wang, J.; Pérez-Jiménez, M.J. (2015); Fault diagnosis of electric power systems based on fuzzy reasoning spiking neural P systems, *IEEE Trans on Power Syst*, 30(3), 1182–1194, 2015.

[38] Wang, T.; Zeng, S.; Zhang, G.; Pérez-Jiménez, M.J.; Wang, J. (2015); Fault section estimation of power systems with optimization spiking neural P systems, *Rom J Inf Sci Technol*, 18(3), 240–255, 2015.

[39] Wang, T.; Zhang, G.; Pérez-Jiménez, M.J.; Cheng, J. (2015); Weighted fuzzy reasoning spiking neural P systems: application to fault diagnosis in traction power supply systems of high-speed railways, *J Comput Theor Nanosci*, 12(7), 1103–1114, 2015.

[40] Wu, T.; Zhang, Z.; Pan, L. (2016); On languages generated by cell-like spiking neural P systems, *IEEE Trans Nanobiosci*, 15(5), 455–467, 2016.

[41] Wei, X.; Yang, D. (2015); An adaptive fault line selection method based on wavelet packet comprehensive singular value for small current grounding system, *Proc. ICDRPT*, 1110–1114, 2015.

[42] Xiong, G.; Shi, D.; Zhu, L.; Duan, X. (2013); A new approach to fault diagnosis of power systems using fuzzy reasoning spiking neural P systems, *Math Probl Eng*, 2013(1), 211–244, 2013.

[43] Yao, Y.Y. (2001); Information granulation and rough set approximation, *Int J Intell Syst*, 16(1), 87–104, 2001.

[44] Zhang, G.; Cheng, J.; Gheorghe, M.; Meng, Q. (2013); A hybrid approach based on differential evolution and tissue membrane systems for solving constrained manufacturing parameter optimization problems, *Appl Soft Comput*, 13(3), 1528–1542, 2013.

[45] Zhang, G.; Rong, H.; Neri, F., Pérez-Jiménez, M.J. (2014); An optimization spiking neural P system for approximately solving combinatorial optimization problems, *Int J Neural Syst*, 24(05), 1440006, 2014.

[46] Zhang, G.; Gheorghe, M.; Pérez-Jiminez, M.J. (2017); *Real-life applications with membrane computing*, Springer International Publishing, Berlin, 2017.

[47] Zhou, Z.; He, J.; Li, X.; Zou, Y. (2006); Research on the novel comprehensive fault line selection method for the NUGS based on the fuzzy theory, *Proc. ICPST*, 1–6, 2006.